

## Ring Dark Solitons and Vortex Necklaces in Bose-Einstein Condensates

G. Theocharis,<sup>1</sup> D. J. Frantzeskakis,<sup>1</sup> P. G. Kevrekidis,<sup>2</sup> B. A. Malomed,<sup>3</sup> and Yuri S. Kivshar<sup>4</sup>

<sup>1</sup>*Department of Physics, University of Athens, Panepistimiopolis, Zografos, Athens 15784, Greece*

<sup>2</sup>*Department of Mathematics and Statistics, University of Massachusetts, Amherst, Massachusetts 01003-4515*

<sup>3</sup>*Department of Interdisciplinary Studies, Faculty of Engineering, Tel Aviv University, Tel Aviv 69978, Israel*

<sup>4</sup>*Nonlinear Physics Group, Research School of Physical Sciences and Engineering, Australian National University, Canberra ACT 0200, Australia*

(Received 7 October 2002; published 26 March 2003)

We introduce the concept of ring dark solitons in Bose-Einstein condensates. We show that relatively shallow rings are not subject to the snake instability, but a deeper ring splits into a robust ringlike cluster of vortex pairs, which performs oscillations in the radial and azimuthal directions, following the dynamics of the original ring soliton.

DOI: 10.1103/PhysRevLett.90.120403

PACS numbers: 03.75.Lm, 05.45.Yv

Intensive studies of Bose-Einstein condensates (BECs) [1] have drawn much attention to the dynamics of nonlinear excitations such as bright [2] and dark [3–5] solitons. In particular, dark solitons in BECs were studied in detail [6], and it was found that they are subject to dynamical and thermal instabilities [7]. The experimentally observed dynamical instability [4] is due to their quasi-1D character: when embedded in a higher dimension, a dark-soliton stripe becomes unstable against transverse snaking [5,8].

Transverse perturbations of dark solitons were extensively studied in nonlinear optics (where such solutions exist in the case of defocusing nonlinearity) [9]. Since the wave number band of the snake instability is limited by a maximum wave number  $Q_m$ , the instability can be suppressed by bending a soliton stripe to close it into an annulus of length  $L < 2\pi/Q_m$ . The resulting *ring dark solitons* (RDS's, i.e., annular troughs on a uniform background), first introduced in Ref. [10], were studied in optics theoretically [11] and experimentally [12]. Note that bright solitons are unstable to collapse in higher dimensions [9], which also pertains to bright ring-shaped structures.

In this Letter, we introduce the concept of RDS in BEC, as a novel class of solitons which can be experimentally created by means of known phase-engineering techniques [12,13]. A principal difference from optics is that the RDS dynamics in BEC is *temporal*, while in optical media it is of the spatial type [10]. Physical means available to control BEC, such as dc and ac magnetic fields, are also completely different from those employed in optics. Using the perturbation theory [14] and simulations, we demonstrate that shallow RDS's in BEC are long-lived objects, that may be observed experimentally on a relevant time scale. On the contrary, deep RDS's are subject to snake instability, splitting into ring-shaped vortex arrays ("vortex necklaces") that, eventually, reduce to four vortex-antivortex pairs, which perform robust double-oscillatory motion in radial and azimuthal directions. All these dynamical features are drastically

different from those known in optics, showing that the concept of RDS comprises a much broader range of behaviors than it was known previously. Moreover, we establish a link of RDS in BEC to ring fluxons in large-area Josephson junctions [15,16].

The evolution of the BEC is governed by the Gross-Pitaevskii equation with a trapping potential  $V(\mathbf{r})$  [1]. We consider a disk-shaped trap of the form  $V(r, z) = m(\omega_r^2 r^2 + \omega_z^2 z^2)/2$ , where  $r^2 = x^2 + y^2$ ,  $m$  is the atom mass,  $\omega_{r,z}$  are the confinement frequencies in the radial and axial directions, and  $\Omega \equiv \omega_r/\omega_z \ll 1$ . Then, following Refs. [17], one can derive an equation for a normalized mean-field wave function  $u(t, r)$ :

$$iu_t = -(1/2)\nabla^2 u + |u|^2 u + (1/2)\Omega^2 r^2 u. \quad (1)$$

We seek for solutions to Eq. (1) describing rings of lower density on a background, which is described by the Thomas-Fermi (TF) approximation. For Eq. (1), the latter is  $u_0 = \sqrt{\mu - (1/2)\Omega^2 r^2} \exp(-i\mu t)$ , where  $\mu$  is the chemical potential. As  $\Omega$  is small, we can define a region where the trapping potential is much smaller than  $\mu$ , then  $u_0(r, t) \approx [\sqrt{\mu} - (1/4\sqrt{\mu})(\Omega r)^2] \exp(-i\mu t)$ . To describe the dynamics of RDS on top of the background  $u_0$ , we look for a solution of Eq. (1) in the form  $u \equiv u_0(r, t)v(r, t)$ , where the complex field  $v(r, t)$  will introduce the ring soliton. For  $\Omega \ll 1$ , the most interesting case is when the radius of the ring is large enough, so that  $1/r = O(\Omega)$ . In this case, upon redefining  $t \rightarrow \mu t$ ,  $r \rightarrow \sqrt{\mu} r$ , Eq. (1) leads to an effective perturbed nonlinear Schrödinger (NLS) equation,

$$iv_t + (1/2)v_{rr} - (|v|^2 - 1)v = P(v), \quad (2)$$

where  $P$  stands for the effective perturbation,

$$P(v) \equiv \mu^{-1}[(1 - |v|^2)vW(r) + (1/2)W'(r)v_r - \sqrt{\mu}(2r)^{-1}v_r],$$

with  $W(r) \equiv (\Omega r)^2/2$ , all terms in the perturbation  $P$  being on the same order of smallness.

We apply the perturbation theory for dark solitons [14] to Eq. (2). We start with the unperturbed dark-soliton and seek for a ringlike solution to Eq. (2) as  $v(r, t) = \cos\varphi(t) \cdot \tanh\xi + i \sin\varphi(t)$ , where  $\xi \equiv \cos\varphi(t)[r - R(t)]$ , and  $\varphi(t)$  and  $R(t)$  are slowly varying phase ( $|\varphi| < \pi/2$ ) and radius of the ring soliton. It is straightforward to derive perturbation-induced evolution equations:

$$\frac{d\varphi}{dt} = -\frac{\cos\varphi}{2\mu} \frac{dW}{dR} + \frac{\cos\varphi}{3\sqrt{\mu}R}, \quad \frac{dR}{dt} = \sin\varphi. \quad (3)$$

Combining these, we arrive at an equation of motion for the RDS radius:

$$\frac{d^2R}{dt^2} = \left[ -\frac{1}{2} \frac{dW(R)}{dR} + \frac{1}{3R} \right] \left[ 1 - \left( \frac{dR}{dt} \right)^2 \right], \quad (4)$$

in which we set  $\mu \equiv 1$ , as  $\mu$  can be eliminated from Eqs. (3) by the transformation  $t \rightarrow \sqrt{\mu}t$ ,  $\Omega \rightarrow \sqrt{\mu}\Omega$ .

In the limiting case of a plane soliton,  $R \rightarrow \infty$ , and with  $\cos\varphi \approx 1$ , Eq. (4) reduces to an equation of motion for the soliton's radius,  $d^2R/dt^2 + (\Omega/2)R = 0$ , which recovers a known result for a quasi-1D dark-soliton in a parabolic potential [6]: it oscillates in a harmonic trap with the frequency  $\Omega/\sqrt{2}$ . On the other hand, in the absence of the trapping potential  $V$  and for an almost black (deepest) soliton, Eq. (4) demonstrates that the curvature-induced effective potential is  $U = -(1/3)\ln R$ , which recovers a result known in the context of nonlinear optics [10]. In the present case, a combination of the trapping potential and ring curvature gives rise to an effective potential well for the soliton's radial degree of freedom,  $\Pi(R) = (1/2) \times (\Omega R)^2 - (1/3)\ln R$ , that resembles oscillations of a circular sine-Gordon (sG) kink in an axially symmetric anti-trap potential, which is possible in large-area Josephson junctions [16] (without the antitrap potential, the circular sG kink periodically collapses and bounces back, forming an extremely robust *pulson* [15]).

The above consideration shows that RDS's can be found in BEC both as oscillating rings and stationary ones, trapped at the bottom of the potential well  $\Pi(R)$ , i.e., with the radius  $R_0 = \Omega^{-1}\sqrt{2/3}$ . For the oscillatory states, the points  $R_{\min}$  and  $R_{\max}$  between which  $R(t)$  oscillates can be found, using Eqs. (3) to eliminate  $\sin^2\varphi$ :  $R_{\min, \max} = [-(2/3)w(k, \eta)]^{1/2}\Omega^{-1}$ , where  $w(k, \eta)$  is the Lambert's  $w$  function defined as the inverse of  $\eta(w) = w \exp(w)$  [18], the integer  $k$  is the branch number of the function ( $k = 0$  and  $k = -1$  correspond to  $R_{\min}$  and  $R_{\max}$ , respectively), and  $\eta \equiv -3W[R(0)] \cos^6\varphi(0) \times \exp\{-3W[R(0)]\}$ .

The possible existence of the stationary and oscillating ring solitons is specific to BECs, where they are supported by the trapping potential, while their counterparts in nonlinear optics expand indefinitely [10]. Stability of the ring solitons, trapped at or around  $R = R_0$ , against transverse perturbations should be tested in direct simulations.

We integrated Eq. (1) numerically, with an initial configuration (IC)

$$u(r, 0) = (1 - \Omega^2 r^2/4)[\cos\varphi(0) \tanh Z(r) + i \sin\varphi(0)],$$

where  $Z(r) = (r - R_0)\cos\varphi(0)$ ,  $\Omega = 0.028$ ,  $R_0 = 28.9$ , and  $\cos\varphi(0)$  is the depth of the input soliton. The cases of oscillating and stationary RDS can be considered, taking  $\cos\varphi(0) \neq 1$  and  $\cos\varphi(0) = 1$ , respectively. Simulations verify that both oscillating and stationary RDS's exist, and their dynamics can be effectively described by Eq. (4), up to a certain time. Then, instabilities develop: RDS either slowly decays into radiation [for  $\cos\varphi(0) < 0.67$ ], or, for  $\cos\varphi(0) \geq 0.67$ , snaking sets in, leading to formation of vortex-antivortex pairs arranged in a robust ring-shaped array (vortex cluster).

To illustrate these generic scenarios, we first take the case with  $\cos\varphi(0) = 0.6$  and  $\sin\varphi(0) = -0.8$ . The corresponding initial structure is shown in Figs. 1(a) and 1(b). According to the analytical results, in this case RDS is expected to oscillate with the period  $T = 240$  between widely different limits,  $R_{\min} = 3.8$  and  $R_{\max} = 69.7$ , the latter being almost at the rim of the BEC cloud, whose TF radius is  $\approx 70$ . It is indeed observed that RDS initially shrinks, attains the maximum contrast at  $R = R_{\min}$  [Fig. 1(c)], and bounces back. After reaching  $R_{\max}$  and bouncing from it, RDS starts to emit radiation in the form of shallow concentric dark rings, as shown in Fig. 1(d). Because of the radiation loss, RDS becomes shallower and, as a result, it accelerates, decreasing the period of the oscillations. We observed that RDS performed at least three complete cycles of the oscillations before final decay, which occurs at  $t \approx 400$ . Qualitatively, this dynamical instability resembles that of a stripe (rectilinear) dark-soliton in BECs [7].

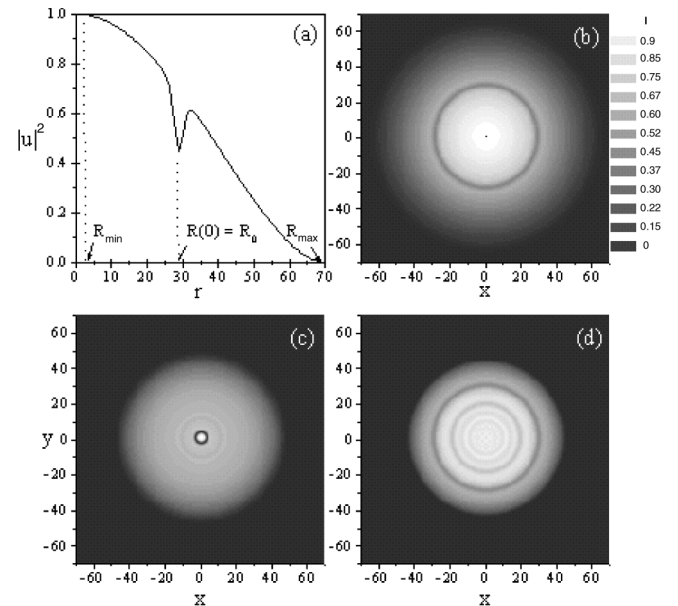


FIG. 1. Evolution of a ring dark soliton (RDS) with  $R(0) = 28.9$  and  $\cos\varphi(0) = 0.6$ . (a),(b) The initial profile shown by cross-section and gray-scale density plots, where RDS corresponds to a gray ring. (c) RDS shrinks to the minimum radius (at  $t = 40$ ). (d) Beginning of the emission of dark concentric rings (at  $t = 160$ ).

To translate the results into units relevant to the experiment [3,4], we assume a  $^{87}\text{Rb}$  condensate of radius  $30\ \mu\text{m}$ , containing 20000 atoms in a disk-shaped trap with  $\omega_r = 2\pi \times 18\ \text{Hz}$  and  $\omega_z = 2\pi \times 628\ \text{Hz}$ . In this case, the RDS considered above has the radius  $R_0 = 12.4\ \mu\text{m}$ , it starts to emit radiation at  $t \approx 40\ \text{ms}$ , and finally decays at  $t = 100\ \text{ms}$ . This time scale is much larger than the lifetime of the dark stripe observed in Refs. [3,4], hence moderately shallow RDS's can be observed too.

Deep RDS's develop the snake instability, which results in the formation of vortex pairs in multiples of four, namely 4 [for  $0.67 \leq \cos\varphi(0) < 0.8$ ], 8 [for  $0.8 \leq \cos\varphi(0) < 0.9$ ], 12 [for  $0.9 \leq \cos\varphi(0) < 0.95$ ], or 16 [for  $0.95 \leq \cos\varphi(0) \leq 1$ ]. Originally, all the pairs are set along a single ring, creating a necklacelike structure. The subsequent evolution of the necklaces is characterized by a transient stage, when quartets of pairs are successively expelled off the necklace, drift inward to the center of the condensate and disappear there. Eventually, there remains a pattern consisting of precisely four vortex pairs. They are arranged along a ring that slowly oscillates between  $R_{\min}$  and  $R_{\max}$ , i.e., the same limits between which the initial RDS oscillated prior to the onset of the instability. Simultaneously, the vortices and antivortices perform an oscillatory motion along the ring, so that the configuration periodically switches between x- and +-like shapes.

The robust necklace patterns consisting of vortex pairs resemble stable clusters of globally linked vortices (of one sign, rather than of the vortex-antivortex type) that were recently found in a 2D BEC model [19]; however, the number of vortices in those clusters could be arbitrary (at least, 2, 4, and 8). Another similar object are necklace soliton clusters in nonlinear optics, which, however, are not stationary, gradually expanding [20] or rotating [21].

The double-oscillatory state persists for long times, typically up to  $t \approx 2000$  (which is  $\approx 500\ \text{ms}$  for the typical case specified above); still later, due to significant distortion of the condensate as a whole, all the vortex pairs annihilate. To illustrate these scenarios, we display two cases, which correspond to situations where the instability initially creates the minimum (4) or maximum (16) number of vortex pairs.

First, we consider RDS with  $\cos\varphi(0) = 0.76$  and  $R_{\min} = 8$ ,  $R_{\max} = 58$ . This IC is very similar to that in Fig. 1(b). It initially shrinks and attains  $R = R_{\min}$  [as in Fig. 1(c)]. After bouncing and subsequently expanding to the rim of the BEC cloud, it starts snaking [see Fig. 2(a)], which is a precursor of splitting. Finally, it splits into four vortex pairs; see Fig. 2(b). The persistent quartet of the pairs arranges itself in a ring configuration. The ring performs slow radial oscillations between  $R_{\min}$  and  $R_{\max}$  with a period  $T \approx 400$  ( $\approx 100\ \text{ms}$ ) up to  $t \approx 2000$ . Simultaneously, the vortices and antivortices move along the ring, so that they form an x-like configuration at  $R =$

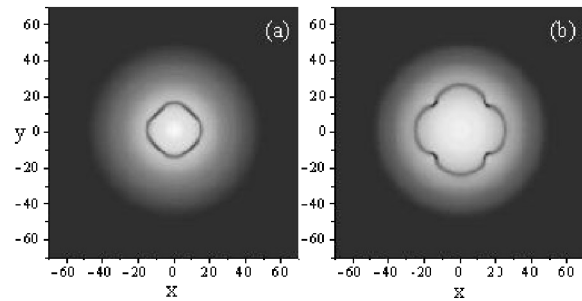


FIG. 2. Evolution of RDS with  $R(0) = 28.9$  and  $\cos\varphi(0) = 0.76$ . (a) Spontaneous undulations developed on the ring at  $t = 60$ . (b) Four vortex pairs are formed, at  $t = 70$ .

$R_{\max}$  [Fig. 3(a)], then an octagon [Fig. 3(b)], and then a +-like pattern. As is seen in Fig. 3(c), the latter one shrinks to  $R = R_{\min}$ , then it bounces and expands, attaining  $R = R_{\max}$  [Fig. 3(d)], and evolves into the x-like pattern, and then the cycle repeats itself.

Finally, we consider the evolution of a black ring soliton, with  $\cos\varphi(0) = 1$ , which, according to the analytical prediction, is expected to be stationary [the corresponding initial state looks similar to that shown in Fig. 1(b)]. First, this configuration indeed remains stationary. However, Fig. 4(a) shows that, at  $t = 40$  ( $\approx 10\ \text{ms}$ ), the ring starts to snake, which ends up with formation of a necklace array of 16 vortex pairs along the ring  $R = R_0$ ; see Fig. 4(b). The subsequent evolution of the necklace results in annihilation of eight pairs, which

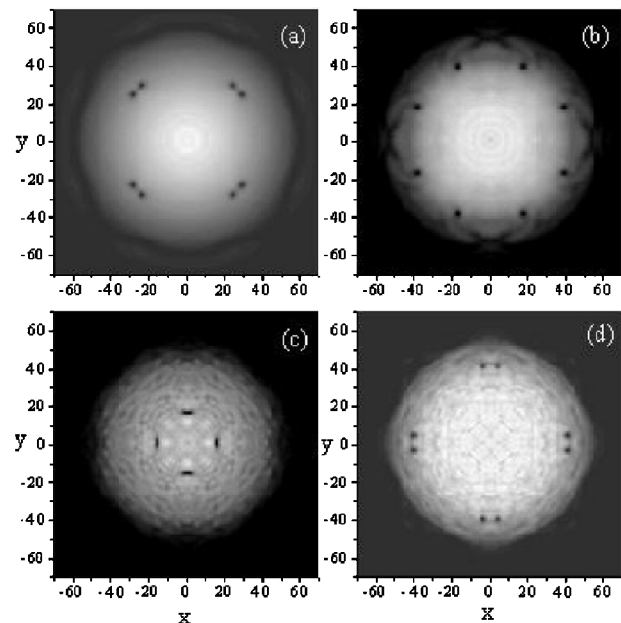


FIG. 3. Evolution of four vortex pairs created by the instability of RDS from Fig. 2 for (a)  $t = 120$ , (b)  $t = 240$ , (c)  $t = 420$ , and (d)  $t = 540$ . The vortex pairs remain on the ring and move along it, so that the configuration oscillates between the x- and +-like configurations, while the ring itself periodically shrinks and expands between  $R_{\min}$  and  $R_{\max}$ .

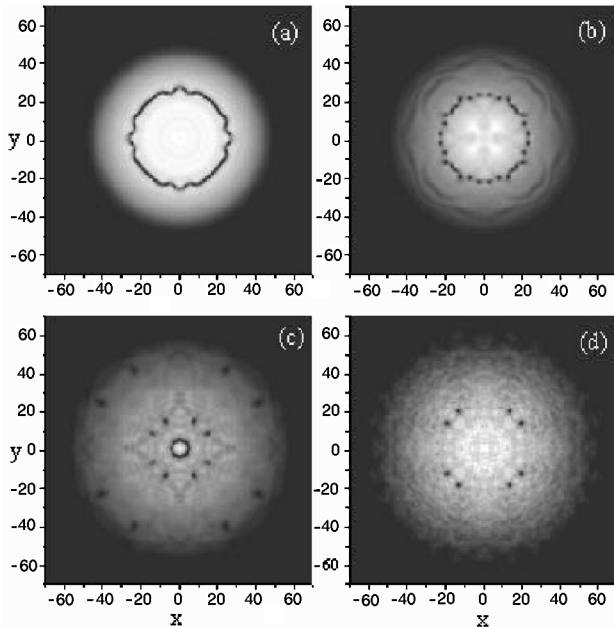


FIG. 4. Evolution of an original stationary ring soliton with  $\cos\varphi(0) = 1$  and  $R(0) = R_0 = 28.9$ . The initial configuration remains undistorted up to  $t = 40$ . (a) Undulations of RDS at  $t = 40$ . (b) Sixteen vortex pairs, formed by  $t = 60$  as a result of the snake instability. Further snapshots are shown for (c)  $t = 240$  and (d)  $t = 760$ . The initial set of 16 vortex pairs reduces first to 12, then to 8, and eventually to 4 pairs, through successive annihilations. Four surviving vortex pairs stay at  $r = R_0$ , oscillating between the  $x$ - and  $+$ -like patterns.

occurs in two steps. At first, four pairs drift inward, where they disappear [Fig. 4(c)], leaving a nearly rectangular array of 12 vortex pairs. Next, the 12-pair pattern expunges two quartets of vortex pairs. One quartet again moves inward and disappears near the center, the other one drifts outward, while four vortex pairs stay at  $R = R_0$ ; see Fig. 4(c). Then, the four outward-moving vortex pairs bounce from the rim of the condensate and move back inward, past the quartet that stays put at  $R = R_0$ , and eventually disappear at the center. Thus, there remains a pattern consisting of four vortex pairs, which still reside at  $R \approx R_0$ ; see Fig. 4(d) (due to the overall distortion of the condensate at this late stage of the evolution,  $R_0$  was properly adjusted). The vortices and antivortices from these pairs move along the ring, so that the configuration performs very slow oscillations between the  $x$ - and  $+$ -like shapes. We have observed almost three complete cycles of such oscillations with the period  $T \approx 500$  ( $\approx 125$  ms).

In conclusion, we have introduced the concept of ring dark solitons in Bose-Einstein condensates, and predicted the existence of both oscillatory and stationary solitons. Simulations show that perturbation theory accurately describes the unperturbed RDS dynamics. However, instabilities gradually set in and, as a result, shallow RDS's slowly decay, while deeper ones develop the snake

instability. In the latter case, a necklace array consisting of vortex-antivortex pairs appears, the number of pairs being a multiple of 4. Eventually, it relaxes to a set of four pairs which sit on a ring oscillating in the radial direction between the same limits which confined the oscillations of the original RDS; simultaneously, the pairs perform oscillatory motion along the ring.

This work was supported by the Special Research Account of the University of Athens (G.T., D.J.F.), a UMass FRG and NSF-DMS-0204585 (P.G.K.), Binational (U.S.-Israel) Science Foundation under Grant No. 1999459 (B.A.M.), and the Australian Research Council (Y.S.K.). Discussions with H.E. Nistazakis are acknowledged.

- 
- [1] F. Dalfovo *et al.*, Rev. Mod. Phys. **71**, 463 (1999).
  - [2] K.E. Strecker *et al.*, Nature (London) **417**, 150 (2002); L. Khaykovich *et al.*, Science **296**, 1290 (2002).
  - [3] S. Burger *et al.*, Phys. Rev. Lett. **83**, 5198 (1999).
  - [4] J. Denschlag *et al.*, Science **287**, 97 (2000).
  - [5] B.P. Anderson *et al.*, Phys. Rev. Lett. **86**, 2926 (2001).
  - [6] W.P. Reinhardt and C.W. Clark, J. Phys. B **30**, L785 (1997); Th. Busch and J.R. Anglin, Phys. Rev. Lett. **84**, 2298 (2000).
  - [7] P.O. Fedichev, A.E. Muryshev, and G.V. Shlyapnikov, Phys. Rev. A **60**, 3220 (1999); G. Huang, J. Szeftel, and S. Zhu, Phys. Rev. A **65**, 053605 (2002); A. Muryshev *et al.*, Phys. Rev. Lett. **89**, 110401 (2002).
  - [8] D.L. Feder *et al.*, Phys. Rev. A **62**, 053606 (2000); J. Brand and W.P. Reinhardt, Phys. Rev. A **65**, 043612 (2002).
  - [9] See Yu.S. Kivshar and D.E. Pelinovsky, Phys. Rep. **331**, 117 (2000), and references therein.
  - [10] Yu.S. Kivshar and X. Yang, Phys. Rev. E **50**, R40 (1994).
  - [11] A. Dreischuh, V. Kamenov, and S. Dinev, Appl. Phys. B **62**, 139 (1996); D.J. Frantzeskakis and B.A. Malomed, Phys. Lett. A **264**, 179 (1999); H.E. Nistazakis *et al.*, Phys. Lett. A **285**, 157 (2001).
  - [12] D. Neshev *et al.*, Appl. Phys. B **64**, 429 (1997); A. Dreischuh *et al.*, Phys. Rev. E **66**, 066611 (2002).
  - [13] L. Dobrek *et al.*, Phys. Rev. A **60**, R3381 (1999); G. Andreiczuk *et al.*, Phys. Rev. A **64**, 043601 (2001).
  - [14] Yu.S. Kivshar and B. Luther-Davies, Phys. Rep. **298**, 81 (1998).
  - [15] J. Geicke, Phys. Scr. **29**, 431 (1984).
  - [16] E.M. Maslov, Physica (Amsterdam) **15D**, 433 (1985).
  - [17] V.M. Pérez-García, H. Michinel, and H. Herrero, Phys. Rev. A **57**, 3837 (1998); L. Salasnich, A. Parola, and L. Reatto, Phys. Rev. A **65**, 043614 (2002); Y.B. Band, I. Towers, and B.A. Malomed, Phys. Rev. A **67**, 023602 (2003).
  - [18] R.M. Corless *et al.*, Adv. Comput. Math. **5**, 329 (1996).
  - [19] L.-C. Crasovan *et al.*, Phys. Rev. E **66**, 036612 (2002).
  - [20] M. Soljačić, S. Sears, and M. Segev, Phys. Rev. Lett. **81**, 4851 (1998); M. Soljačić and M. Segev, Phys. Rev. Lett. **86**, 420 (2001).
  - [21] A.S. Desyatnikov and Yu.S. Kivshar, Phys. Rev. Lett. **88**, 053901 (2002).